Comparison of three magnetopause prediction models under extreme solar wind conditions

Y.-H. Yang,[1] J. K. Chao,[1] C.-H. Lin,[1,2] J.-H. Shue,[3] X.-Y. Wang,[4] P. Song,[5]
C. T. Russell,[6] R. P. Lepping,[7] and A. J. Lazarus[8]

Received 12 March 2001; revised 17 July 2001; accepted 17 July 2001; published 5 January 2002.

[1] A database, the largest one to date, of magnetosheath encounters by geosynchronous satellites during 1986–1992 and 1999–2000 and upstream observations by Wind, IMP 8, or Geotail in the solar wind are used to estimate the forecasting capability of the models of *Chao et al.* [2001], *Shue et al.* [1998], and *Petrinec and Russell* [1996]. For each of the 1-min resolution data points obtained by GOES spacecraft, we check the following two things: if the magnetosheath was observed by the spacecraft, and if each of the three models predicted a magnetosheath encounter by the spacecraft. Three parameters are defined to quantify the models' forecasting capability: probability of prediction (PoP), probability of detection (PoD), and false alarm rate (FAR). A higher PoP and PoD with a lower FAR imply a better forecasting model. In the 1986–1992 period we found that most of the magnetosheath encounters observed at 6.6 R_E are detected. In particular, the *Chao et al.* [2001] model predicts the lowest FAR compared with those of the other two models. We have also studied the magnetosheath encounters made by GOES spacecraft for the period from 1999 to 2000 using Wind and Geotail as the solar wind monitor. This independent database of magnetosheath encounters during 1999–2000 confirms our previous anticipations. The PoD of *Petrinec and Russell* [1996] model (94%) is much higher than those of *Shue et al.* [1998] (74%) and *Chao et al.* [2001] (84%) models. The *Chao et al.* [2001] model has a higher PoP than the other two models. The values of FAR for *Chao et al.* [2001], *Shue et al.* [1998], and *Petrinec and Russell* [1996] models are 25, 27, and 40%, respectively. *INDEX TERMS:* 2722 Magnetospheric Physics: Forecasting; 2724 Magnetospheric Physics: Magnetopause, cusp, and boundary layers

1. Introduction

[2] The magnetopause plays an important role in protecting Earth from the intense solar wind. Under normal solar wind conditions the subsolar point of the magnetopause is generally located at ~10 R_E from Earth. Under extreme solar wind conditions, namely, a large southward interplanetary magnetic field (IMF, B_z) and/or a high solar wind dynamic pressure (D_p), the magnetopause can move inside geosynchronous orbit (6.6 R_E). At that time, geosynchronous satellites that use the local magnetic field for orientation information may become misoriented in the randomly directed field in the magnetosheath.

[3] *Chapman and Ferraro* [1931] first suggested the existence of a magnetopause boundary. They proposed that dynamic pressure D_p is the factor that controls the location of the magnetopause. On January 14, 1967, the magnetopause was first detected to penetrate within geosynchronous orbit by the ATS 1 satellite [*Opp*, 1968; *Cummings and Coleman*, 1968, and references therein]. *Aubry et al.* [1970] suggested that erosion of magnetic flux from the dayside magnetosphere to the tail also results in an inward motion of the magnetopause during southward IMF. The *Fairfield* [1971] study of magnetopause crossings supported this suggestion and showed that more earthward crossings are associated with larger southward IMF. Fairfield's study did not include any geosynchronous magnetopause crossings. *Russell* [1976] first analyzed geosynchronous magnetopause crossings systematically by using two years (1966–1968) of magnetic field data from ATS 1. His study showed that the magnetopause crosses inside of geosynchronous orbit ~0.3% of the time. On the basis of studies of geosynchronous magnetopause crossings identified from the magnetometer data of GOES 2, 5, and 6 between 1978 and 1986, *Rufenach et al.* [1989] found that both a high D_p and a large southward IMF are required for the magnetopause to move inside 6.6 R_E. Later, *McComas et al.* [1993, 1994] used particle data to identify crossings at geosynchronous orbit.

[4] Many magnetopause models have been proposed in the past [*Fairfield*, 1971; *Holzer and Slavin*, 1978; *Formisano et al.*, 1979; *Sibeck et al.*, 1991; *Petrinec et al.*, 1991; *Petrinec and Russell*, 1993, 1996; *Roelof and Sibeck*, 1993; *Shue et al.*, 1997, 1998; *Kuznetsov and Suvorova*, 1998a, 1998b; *Kawano et al.*, 1999], but few papers have studied the forecasting capability of such models for geosynchronous magnetopause crossings. Recently, *Shue et al.* [2000] discussed the applicability of each of the magnetopause models and found the *Shue et al.* [1998] model (SM) and *Petrinec and Russell* [1996] model (PRM) to be the most suitable for extreme solar wind conditions. *Shue et al.* [2000] used the subsolar distance r_0 to check whether the predicted magnetopause location

[1]Institute of Space Science, National Central University, Chung-Li, Taiwan.
[2]Also at Department of Electrical Engineering, Nan-Jeon Institute of Technology, Yen-Shui, Taiwan.
[3]Applied Physics Laboratory, Johns Hopkins University, Laurel, Maryland, USA.
[4]Center for Space Science and Applied Research, Academic Sinica, Beijing, China.
[5]Center for Atmospheric Research, University of Massachusetts, Lowell, Massachusetts, USA.
[6]Institute of Geophysics and Planetary Physics, University of California, Los Angeles, California, USA.
[7]Laboratory for Extraterrestrial Physics, NASA Goddard Space Flight Center, Greenbelt, Maryland, USA.
[8]Center for Space Research, Massachusetts Institute of Technology, Cambridge, Massachusetts, USA.

0148-0227/02/2001JA000079$09.00

Table 1. Magnetosheath Encounters on Geosynchronous Orbit With Corresponding Upstream Solar Wind Data During 1986–1992

Year	Month	Day	Satellite	Start Time, UT (LT)	End Time, UT (LT)	Duration, min
1986	2	7	G5	1635 (1139)	1643 (1147)	4, 8
1986	2	7	G5	1645 (1149)	1648 (1152)	1, 3
1986	2	7	G6	1640 (0928)	1643 (0931)	3, 3
1986	2	7	G6	1648 (0936)	1650 (0938)	1, 2
1986	2	8	G5	1522 (1026)	1530 (1034)	4, 8
1986	2	8	G5	1532 (1036)	1543 (1047)	1, 11
1986	2	8	G6	1524 (0812)	1527 (0815)	1, 3
1986	2	8	G6	1531 (0819)	1546 (0834)	2, 15
1989	4	25	G6	2004 (1103)	2019 (1118)	8, 15
1989	4	25	G6	2038 (1137)	2044 (1143)	5, 6
1989	4	25	G7	2002 (1248)	2016 (1302)	5, 14
1990	6	12	G6	1955 (1055)	2157 (1257)	56, 122
1990	6	12	G7	1956 (1305)	2038 (1347)	17, 42
1991	11	21	G6	2039 (1138)	2041 (1:40)	2, 2
1991	11	21	G6	2044 (1143)	2051 (1150)	2, 7
1991	11	21	G7	2045 (1351)	2049 (1355)	1, 4
1992	3	17	G7	1833 (1110)	1851 (1128)	1, 18

is within 6.6 R_E or not. However, it is possible that the magnetopause had already moved inside 6.6 R_E at the subsolar point while geosynchronous satellites were still in the magnetosphere at other local times. They required that individual crossings be separated by 20-min or 60-min intervals, and then they individually calculated the number of crossings. *Chao et al.* [2001] improved the magnetopause crossing database used by *Shue et al.* [1997, 1998] and derived a model (CM) that is to be used for both normal and extreme solar wind conditions.

[5] The purpose of this study is to provide an improved metric for comparing the forecasting capability of the above three models (SM, PRM, and CM) so that a proper magnetopause model can be selected for forecasting space weather and for use in magnetospheric studies. We use the radial distance r to check whether or not the predicted magnetopause crosses geosynchronous orbit and estimate the exact duration in minutes when the GOES spacecraft are in the magnetosheath. Under these circumstances we can distinguish multiple crossings easily. In order to concentrate on the quality of the model predictions of crossings at geosynchronous orbit, we exclude intervals when the solar wind parameters are in their nominal ranges. The magnetosheath encounters made by GOES spacecraft during 1986–1992 and 1999–2000 are compared to the model predictions of them, where the magnetosheath encounters during 1986–1992 have been used as the database of CM. Thus, for an independent comparison of the three models, we estimate a model's forecasting capability for the magnetosheath encounters during 1999–2000. In section 2 we describe the geosynchronous and solar wind data used in this paper. In section 3 we briefly introduce the three magnetopause models compared in this study. In section 4 we present our method for evaluating the forecasting capability of each model. Our results are described in section 5. Discussions and conclusions are given in sections 6 and 7, respectively.

2. Data Selection

[6] The data of GOES 5, 6, 7, 8, 10, IMP 8, Wind, and Geotail are used in this study, of which only the GOES 5, 6, 7, and IMP 8 data are used to create the CM for extreme solar wind conditions. The GOES spacecraft provide good opportunities to observe the occurrence of crossings at geosynchronous orbit. IMP 8, Wind, and Geotail provide the upstream IMF and plasma data used in this study to obtain predicted magnetopause locations of the PRM, SM, and CM. All of the geomagnetic field and solar wind data are 1-min or 90-s averages, which are more accurate then the 5-min averages used by *Shue et al.* [2000]. By comparing the predicted duration when the magnetopause moves inside 6.6 R_E with the observations of GOES spacecraft, we estimate the models' forecasting capability for magnetosheath encounters at geosynchronous orbit.

2.1. Geosynchronous Data

[7] Under normal solar wind conditions, the GOES spacecraft are in the magnetosphere and measure a northward geomagnetic field. If the magnetopause moves inside geosynchronous orbit owing to an enhanced D_p and a large southward B_z, a GOES spacecraft can be exposed to the magnetosheath environment and observe the IMF. Since it is difficult to identify a crossing from the magnetic field data alone when IMF is northward, the duration when GOES spacecraft observe southward magnetic field is recognized as the period of GOES in the magnetosheath. GOES 5, 6, and 7 were operated during the period 1986–1992, and GOES 8 and 10 were operated during 1999–2000. The geomagnetic field data of 1-min averages from GOES spacecraft are obtained from the National Geophysical Data Center (NGDC). In general, a crossing is identified if the north-south component of the geomagnetic field (H_p) changes its direction suddenly. When the northward (southward) geomagnetic field turns south (north), it means that the magnetopause motion near 6.6 R_E causes a GOES to enter (exit) the magnetosheath. A sudden change in direction of a single data point of H_p is not used to identify a magnetopause crossing.

[8] During 1986–1992 the GOES spacecraft were in the magnetosheath for a total of 4818 min, but only 114-min periods of these had accompanying upstream solar wind parameters. These magnetosheath encounters are shown in Table 1. The first through third columns show the year, month, and day of a crossing, respectively. The fourth column identifies the observing satellites GOES 5, 6, and 7, which are denoted by G5, G6, and G7, respectively. The fifth and sixth columns record the times when the satellite entered (i.e., H_p turned southward) and exited (i.e., H_p turned northward) the magnetosheath, respectively. Local time is given in parentheses. The first number in the seventh column represents the available IMP 8 data in minutes, and the second number represents the total duration when the GOES spacecraft stayed in the magnetosheath. Since the data of Wind and Geotail have much fewer bad data points than that of IMP 8, a total of 1220 min of magnetosheath entering by GOES spacecraft with available solar wind parameters during 1999–2000 (not shown here) is obtained compared to only 114 min obtained during the 1986–

1992. In this study, magnetosheath encounters are selected only when a GOES spacecraft is located in the dayside.

2.2. Solar Wind Data

[9] In our prediction scheme we assume that only B_z and D_p affect the location and shape of the magnetopause. In this study, 1-min averages of IMP 8 and Geotail data and 90-s averages of Wind data are used to calculate D_p, which includes also the helium contribution if it is available to the dynamic pressure. We also consider the time shift (Δt) of the solar wind from IMP 8, Wind, or Geotail to the GOES spacecraft. In general, we let $\Delta t = (x - 6.6)/V_{sw}$, where x is the x location of the IMP 8, Wind, or Geotail position in interplanetary space, 6.6 is the distance of geosynchronous orbit in R_E, and V_{sw} is the x component of the solar wind velocity measured by the solar wind monitors, when the GSM coordinate system is used. However, when the fluctuations associated with the upstream solar wind parameters are large, the predicted time shift can be in error. Therefore we compare the magnetic field variations in the solar wind (IMP 8, Wind, and Geotail) with those in the magnetosheath (GOES) to obtain a more accurate time shift. The response time of the magnetopause to the solar wind change, coming from solar wind-magnetosphere interactions, is not included here. This is equivalent to assuming that the whole magnetopause responds instantaneously when the upstream solar wind parameters reach the subsolar point at 6.6 R_E. Since the size and shape of the magnetopause vary with upstream solar wind conditions, we predict the size and shape of the magnetopause as a function of B_z and D_p under equilibrium conditions. Predictions will not be made under one or more of the following situations: (1) IMP 8, Wind, or Geotail move inside the magnetosheath or magnetosphere, (2) either the data of the GOES spacecraft or the upstream solar wind parameters are unavailable, and (3) the GOES spacecraft are on the magnetosphere's nightside.

3. Models

[10] As mentioned in section 1, studies of the location and shape of the magnetopause have a long history. The applicability of magnetopause models for predicting crossings at 6.6 R_E has been discussed in detail by *Shue et al.* [2000], who compared the forecasting capability of the PRM and SM. In this paper a new magnetopause model, CM, is also included for comparison in addition to the PRM and SM. These three models are introduced briefly as follows.

3.1. *Petrinec and Russell* [1996] Model

[11] Using the ISEE 1 and 2 magnetometer data over a 10-year period and the corresponding solar wind parameters from IMP 8, *Petrinec et al.* [1991] obtained a model for the size and shape of the dayside magnetopause. *Petrinec and Russell* [1993] further developed a model of the near-Earth magnetotail according to the total pressure balance between lobe plasma and the solar wind. By combining their dayside and nightside magnetopause models with a smooth connection at the terminator, *Petrinec and Russell* [1996] derived a model for the entire magnetopause. The functional form of their dayside model is

$$r = \frac{14.63\left(\frac{D_p}{2.1}\right)^{\frac{-1}{6}}}{\left[1 + \left(\frac{14.63}{10.3 + m_1 B_z} - 1\right)\cos\theta\right]},$$

where $m_1 = 0$ for northward IMF and $m_1 = 0.16$ for southward IMF. Here r is the radial distance of the magnetopause, and θ is the solar zenith angle; thus the dayside magnetopause location is independent of B_z for northward IMF.

[12] The nightside magnetopause model has a different functional form. The radial distance r in the nightside is estimated by $r = \sqrt{(X^n)^2 + (R^n)^2}$, where $X^n = r\cos\theta$, $R^n = r\sin\theta$, and superscript n denotes the nightside magnetopause. For a given X^n,

$$R^n = \frac{-2}{0.085}\left[\arcsin\sqrt{2.98(D_p)^{-0.524}\exp^{0.085X^n}(0.152 - m_2 B_z)} - \arcsin\sqrt{2.98(D_p)^{-0.524}(0.152 - m_2 B_z)}\right] + 14.63\left(\frac{D_p}{2.1}\right)^{\frac{-1}{6}},$$

where $m_2 = 0.00137$ for northward IMF and $m_2 = 0.00644$ for southward IMF.

3.2. *Shue et al.* [1998] Model

[13] Selecting the crossings observed by ISEE 1, 2, Active Magnetospheric Particle Tracer Explorers (AMPTE)/Ion Release Module (IRM), and IMP 8, *Shue et al.* [1997] derived a new functional form,

$$r = r_0\left(\frac{2}{1 + \cos\theta}\right)^{\alpha},$$

to describe the location and shape of the magnetopause, where r is the radial distance and θ is the angle between r and the Sun-Earth line (i.e., the solar zenith angle) directions, where Earth is located at the origin. The two parameters of r_0 and α represent the subsolar standoff distance and the level of tail flaring, respectively. For different α this functional form can represent an open- or closed-tail magnetopause. On the basis of the study of the magnetic cloud event of January 11, 1997, *Shue et al.* [1998] modified the dependence of r_0 and α on B_z and D_p and obtained an improved model [*Shue et al.*, 1998]. The newly derived model has the following relationship:

$$r_0 = \{10.22 + 1.29\tanh[0.184(B_z + 8.14)]\}(D_p)^{\frac{-1}{6.6}},$$

$$\alpha = (0.58 - 0.007B_z)[1 + 0.024\ln(D_p)].$$

This model allows a saturation of the southward B_z effect, as can be seen in Figure 1b, where r_0 remains constant for more negative B_z.

3.3. *Chao et al.* [2001] Model

[14] *Chao et al.* [2001] improved the magnetopause crossings' database used by *Shue et al.* [1997, 1998] based on the following considerations. In the original database, for simplicity, the time shift for solar wind propagation from IMP 8 (or ISEE 3) to Earth is assumed to be constant (10 min for IMP 8 and 50 min for ISEE 3). Because the speed of the solar wind can vary substantially especially during the disturbed times we are studying and because the spacecraft locations are not fixed, the transit time can vary by a large amount; therefore *Chao et al.* [2001] use the actual satellite positions and the measured solar wind speed to estimate a more accurate time shift in the database. Magnetopause crossings by geosynchronous spacecraft during 1986–1992 are included so that the database can be used for extreme solar wind conditions. Possible bias due to a satellite's geosynchronous orbit has been minimized in the model of *Chao et al.* [2001] by fitting the $r_0 = 6.6$ R_E contour to the outer boundary of the pluses in Figure 1d, simultaneously requiring the estimated errors of the fitting staying at a minimum value. Thus the coefficients of the model for the extreme solar wind conditions are obtained. Along the flank of the magnetopause, it is difficult to distinguish shocked magnetosheath from unshocked solar wind. In the past some data of IMP 8 have been incorrectly considered to be solar wind values when the satellite was actually in the magnetosheath. Such situations are eliminated in the new database. All crossings are corrected for aberration in the GSM coordinate system. The CM has the same

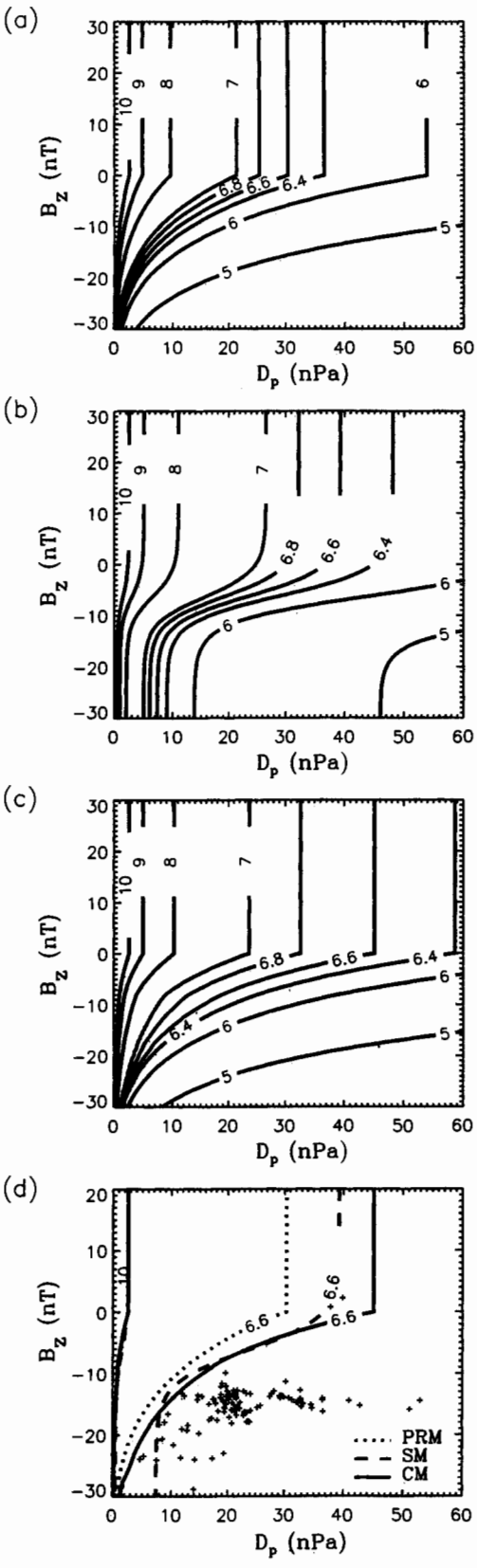

Figure 1. Contours of the subsolar standoff distance r_0 for the models of (a) *Petrinec and Russell* [1996] (PRM), (b) *Shue et al.* [1998] (SM), and (c) *Chao et al.* [2001] (CM), respectively. (d) Comparison of r_0 contours for the PRM (dotted), SM (dashed), and CM (solid). The pluses represent the corresponding B_z and D_p when a GOES spacecraft is in the magnetosheath during 1986–1992.

functional form for the magnetopause as does the SM, but the dependence of r_0 and α on B_z and D_p is different. In order to distinguish magnetopause responses under normal and extreme solar wind conditions, respectively, the dependence of r_0 is derived separately. Those observed crossings with $r > 6.7\ R_E$ and $r \le 6.7\ R_E$ are used to derive a relationship for normal and extreme solar wind conditions, respectively; then the relationships are used as the models for normal and extreme solar wind conditions with $r_0 \ge 7.0\ R_E$ and $r_0 \le 6.4\ R_E$, respectively. For r_0 between 6.4 and 7.0 R_E, interpolation is applied for continuous and smooth transition, where a natural log variation of r_0 with D_p is applied to the region of $r_t \le r_0 < 7.0\ R_E$ and a linear variation of r_0 with D_p is applied to the region of $6.4\ R_E < r_0 < r_t$. It is found that if $r_t = 6.7\ R_E$, we can have a continuous and smooth transition such that neither r_0 nor dr_0/dD_p show a jump at any value of D_p and the dr_0/dD_p is always negative from normal to extreme conditions. The total errors of the best fit with interpolation are found to remain the same as that without an interpolation; then the CM is obtained as follows:

$$r_0 = \begin{cases} (a_1)(D_p)^{\frac{-1}{a_4}} & B_z \ge 0 \\ (a_1 + a_2 B_z)(D_p)^{\frac{-1}{a_4}} & -8 \le B_z < 0 \\ (a_1 + 8a_3 - 8a_2 + a_3 B_z)(D_p)^{\frac{-1}{a_4}} & B_z < -8 \end{cases}$$

$$\alpha = (a_5 + a_6 B_z)(1 + a_7 D_p).$$

[15] Under normal solar wind conditions (i.e., for $r_0 \ge 7.0\ R_E$) the coefficients $a_1 = 11.646$, $a_2 = 0.216$, $a_3 = 0.122$, $a_4 = 6.215$, $a_5 = 0.578$, $a_6 = -0.009$, and $a_7 = 0.012$ are derived, while under extreme conditions (i.e., for $r_0 \le 6.4\ R_E$) the coefficients are $a_1 = 11.646$, $a_2 = 0.169$, $a_3 = 0.158$, $a_4 = 6.800$, $a_5 = 0.578$, $a_6 = -0.009$, and $a_7 = 0.012$. In the region of $6.4\ R_E < r_0 < 7.0\ R_E$, interpolations are applied. The r_0 is independent of B_z when IMF is northward. Note that α needs no interpolation from normal to extreme conditions.

[16] In deriving the CM model for extreme solar wind conditions, the following assumptions have been imposed. First, the functional forms in terms of D_p and B_z for normal and extreme conditions are assumed to be the same except the coefficients are different. Second, the subsolar distances r_0 for $B_z > 0$ depend on D_p only with a power equal to $(-1/a_4)$, where a_4 can be different between normal and extreme conditions. Third, the coefficients a_1, a_5, a_6, and a_7 do not change between normal and extreme conditions. Then, from the magnetosheath encounters shown in Figure 1d, the values of $a_2 = 0.169$, $a_3 = 0.158$, and $a_4 = 6.80$ are obtained by best fitting all the pluses for least errors.

3.4. Characteristics of the PRM, SM, and CM

[17] Figures 1a–1c show the contours of r_0 for various B_z and D_p of the three models. From top to bottom are the PRM, SM, and CM, respectively. It can be seen that r_0 predicted by the PRM is always smaller than those of the SM and CM under the same solar wind conditions; hence it is expected that more periods of GOES in the magnetosheath should be predicted by the PRM. Under a strong southward IMF (e.g., $B_z = -20$ nT) condition, a smaller D_p is needed for the PRM (e.g., $D_p = 1$ nPa) than for the other two models to push the magnetopause inside 6.6 R_E at the subsolar point. The r_0 of the SM is independent of B_z for the same D_p when southward B_z is greater than 20 nT. Under northward IMF, a larger D_p is needed for the CM (e.g., $D_p = 45$ nPa) than the PRM and SM to move the r_0 of the magnetopause to 6.6 R_E. All three models have the characteristic that a larger D_p is needed to push the magnetopause closer to the Earth when r_0 is smaller. Figure 1d shows the comparison of r_0 contours of these three models under normal (i.e., $r_0 = 10\ R_E$) and extreme (i.e., $r_0 = 6.6\ R_E$) solar wind conditions. Dotted, dashed, and solid curves represent the PRM, SM, and CM, respectively. The r_0 contours of three models are similar for normal solar wind

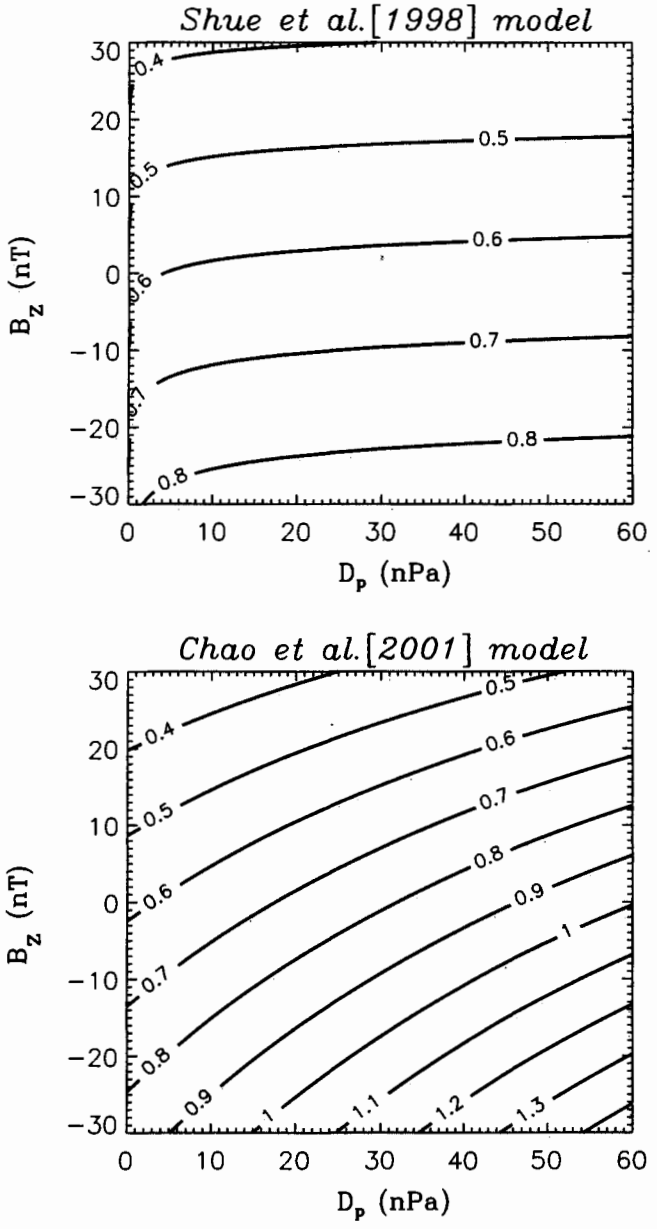

Figure 2. Contours of tail flaring, α, for the SM and CM.

conditions, while their behaviors are different for extreme solar wind conditions. The associated B_z and D_p values of GOES spacecraft in the magnetosheath during 1986–1992 are shown as pluses in Figure 1d. Since the $r_0 = 6.6\ R_E$ contour of CM is obtained from the idea that it should be as close to the outer edge of these pluses as possible, CM has the largest r_0 for most of these pluses.

[18] Contours of α of the SM and CM are plotted, respectively, in Figure 2. The PRM does not contain an α factor, and the tail is assumed to be cylindrical in shape; hence it is not shown here. The α value changes slowly with D_p and B_z for the SM, while for the CM, α changes more sensitively with D_p and B_z.

4. Method of Analysis

[19] Predicting the locations of the magnetopause along the same radial direction as the GOES spacecraft at 1-min resolution is our objective. If the predicted r in the Earth-GOES direction is less than or equal to 6.6 R_E, which means the GOES spacecraft should be inside the magnetosheath, and GOES is (is not) so located, we classify a model's prediction as correct (incorrect). If the predicted r in the Earth-GOES direction is greater than 6.6 R_E, which means the GOES spacecraft should be in the magnetosphere, and GOES is (is not) so located, we also classify a model's prediction as correct (incorrect). We record the predicted crossing times when the magnetopause moves inside or outside geosynchronous orbit, from which the predicted duration of the GOES spacecraft being in the magnetosheath can be obtained, and then, by comparing the observations for each data point, the forecasting capability of each model can be estimated. Comparisons are limited to within 0800–1600 LT, owing to no occurrence of crossings during the nightside. The data resolution of IMP 8, Geotail, and the GOES spacecraft is 1 min, and the Wind is 1.5 min, which is much better than the previous studies, which used 5-min or 1-hour time resolution.

Table 2. The Possible Situations for Observation and Prediction[a]

	Observation Yes	Observation No
Prediction Yes	HT	FAT
Prediction No	MT	CRT

[a] HT, hit time; FAT, false alarm time; MT, miss time; CRT, correct rejection time. Probability of prediction (PoP): HT + CRT/HT + MT + FAT + CRT. Probability of detection (PoD): HT/HT + MT. False alarm rate (FAR): FAT/HT + FAT.

[20] There are four comparison conditions, which are defined in units of minutes (as shown in Table 2): hit time (HT), false alarm time (FAT), miss time (MT), and correct rejection time (CRT). The format is the same as that in Table 3 of *Shue et al.* [2000]. A model has a correct prediction when the predicted periods agree with observations as given in the HT and CRT, while a model has an incorrect prediction as given in the FAT and MT when the predicted periods disagree with observations. The HT refers to the length of time during which predictions are observed. The FAT refers to the length of time during which predictions are not observed. The MT refers to the length of time during which observed sheath encounters have not been predicted. The CRT refers to the length of time during which no sheath encounter is observed nor predicted. TT is the total time satisfying the relation TT = HT + FAT + MT + CRT. TT is the same for all three models. The statistics are done only when the magnetosheath encounters are observed or predicted at least by one of the three models. Consequently, the values of each model's CRT are reduced substantially.

[21] Three parameters are defined from the above four quantities to determine the forecasting capability. They are probability of prediction (PoP), probability of detection (PoD), and false alarm rate (FAR) [*Schaefer*, 1990; *Doswell et al.*, 1990], respectively, where the PoP refers to the percentage of correct forecasting and is defined as (HT + CRT)/TT, the PoD refers to the percentage of successful forecasting for observed sheath encounters and is defined

Table 3a. Prediction Results of the Three Models During 1986–1992[a]

Model	HT	MT	FAT	CRT	TT
Chao et al. [2001]	109	5	238	781	1133
Shue et al. [1998]	106	8	367	652	1133
Petrinec and Russell [1996]	111	3	615	404	1133

[a] Units are minutes.

Table 3b. Prediction Results of the Three Models During 1999–2000[a]

Model	HT	MT	FAT	CRT	TT
Chao et al. [2001]	1027	193	347	1121	2688
Shue et al. [1998]	898	322	324	1144	2688
Petrinec and Russell [1996]	1145	75	774	694	2688

[a] Units are minutes.

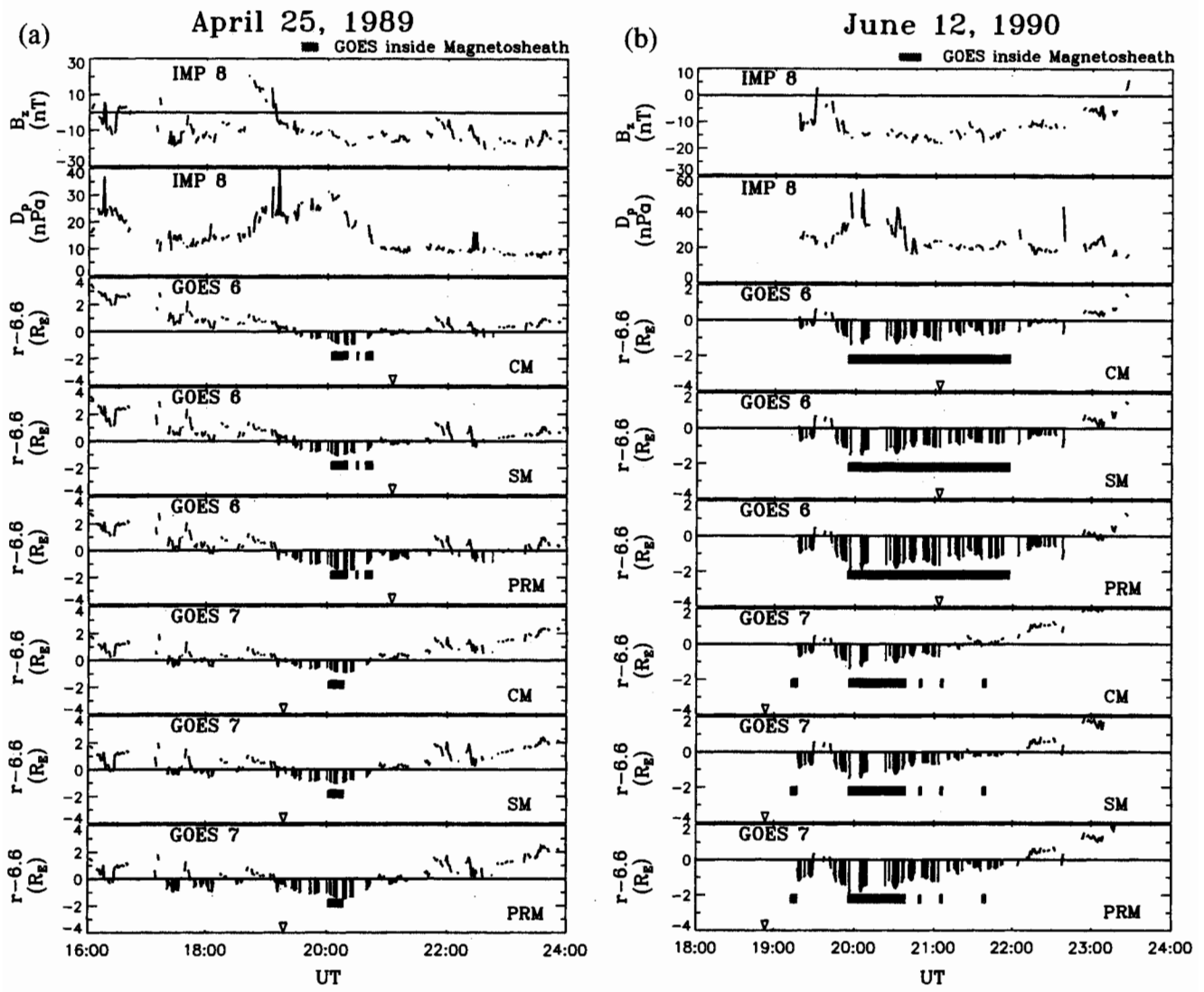

Figure 3. Observations by IMP 8 and predictions by the three models in GOES 6 and 7 locations on (a) April 25, 1989, and (b) June 12, 1990. The black regions denote the periods when predicted magnetopause is within geosynchronous orbit. Hatched bars indicate the GOES spacecraft inside the magnetosheath. The upside-down triangles denote local noon of the GOES spacecraft.

as HT/(HT + MT), and the FAR refers to the percentage of predicted sheath encounters that are not observed and is defined as FAT/(HT + FAT). It is necessary to consider all three parameters at the same time for comparing a model's forecasting capability. Higher PoP represents a better prediction of GOES staying either in the magnetosheath or magnetosphere, while higher PoD represents a better prediction of sheath encounters only. Higher FAR represents less reliable predicted results; therefore higher PoP and PoD with lower FAR represent a better forecasting model.

5. Results

[22] Our comparisons are given for the periods of 1986–1992 and 1999–2000, respectively. Since the relationship of (r_0, α) with (B_z, D_p) of CM for the extreme solar wind conditions is derived from the crossings in the period of 1986–1992, it is likely the CM gives a better prediction than the other two. Therefore an independent database of geosynchronous crossings in the period 1999–2000 is selected for examining the forecasting capability of three models. The predicted results of these two periods are described separately as follows.

5.1. During 1986–1992

[23] Figures 3a and 3b show the IMF B_z and D_p measured by IMP 8 and the predicted results for the crossings on April 25, 1989, and June 12, 1990, respectively. The top two panels show B_z and D_p with time shifted for comparison with GOES data. The next six panels show the differences of radial distances between the predicted magnetopause and the GOES spacecraft (i.e., r = 6.6 R_E) shown as a straight line. The distance differences predicted by the CM, SM, and PRM, respectively, are shown in Figure 3. Black regions are where r is less than 6.6 R_E; thus these regions represent the predicted periods that a GOES should be in the magnetosheath. The hatched bars show the periods that a GOES actually stayed in the magnetosheath. The upside-down triangles indicate when the GOES spacecraft are at local noon. The periods of coexistence between hatched and black regions indicate the HT during which sheath encounters can be detected by models. The periods when hatched bars alone occur refer to the MT during which sheath encounters cannot be detected by models. Periods of black without hatched bars refer to the FAT during which models predict the magnetopause inside 6.6 R_E but the GOES spacecraft is still in the magnetosphere. Periods with-

Table 4a. Comparison of Prediction Capability for the Three Models During 1986–1992[a]

Model	PoP	PoD	FAR
Chao et al. [2001]	79	96	69
Shue et al. [1998]	67	93	78
Petrinec and Russell [1996]	45	97	85

[a]Units are percentage.

Table 4b. Comparison of Prediction Capability for the Three Models During 1999–2000[a]

Model	PoP	PoD	FAR
Chao et al. [2001]	80	84	25
Shue et al. [1998]	76	74	27
Petrinec and Russell [1996]	68	94	40

[a]Units are percentage.

out black and hatched regions refer to the CRT during which no sheath encounter occurs.

[24] Comparing three magnetopause models in Figure 3, we find that the PRM has more black regions than the SM and CM

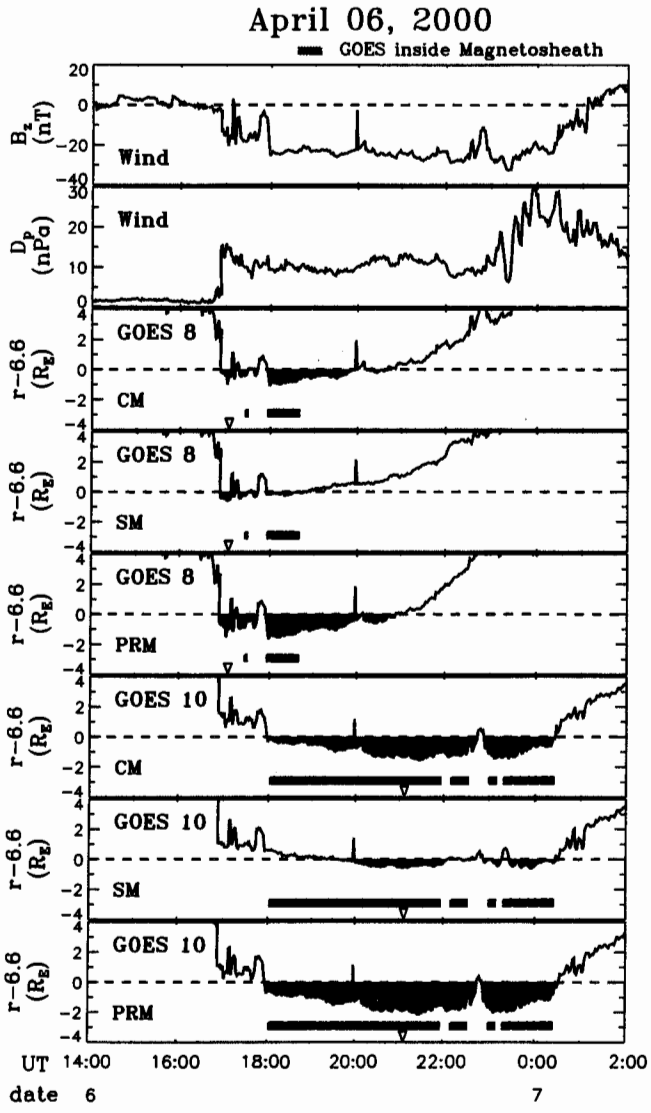

Figure 4. Comparison of predictions and observations on April 6, 2000, in the same format as Figure 3.

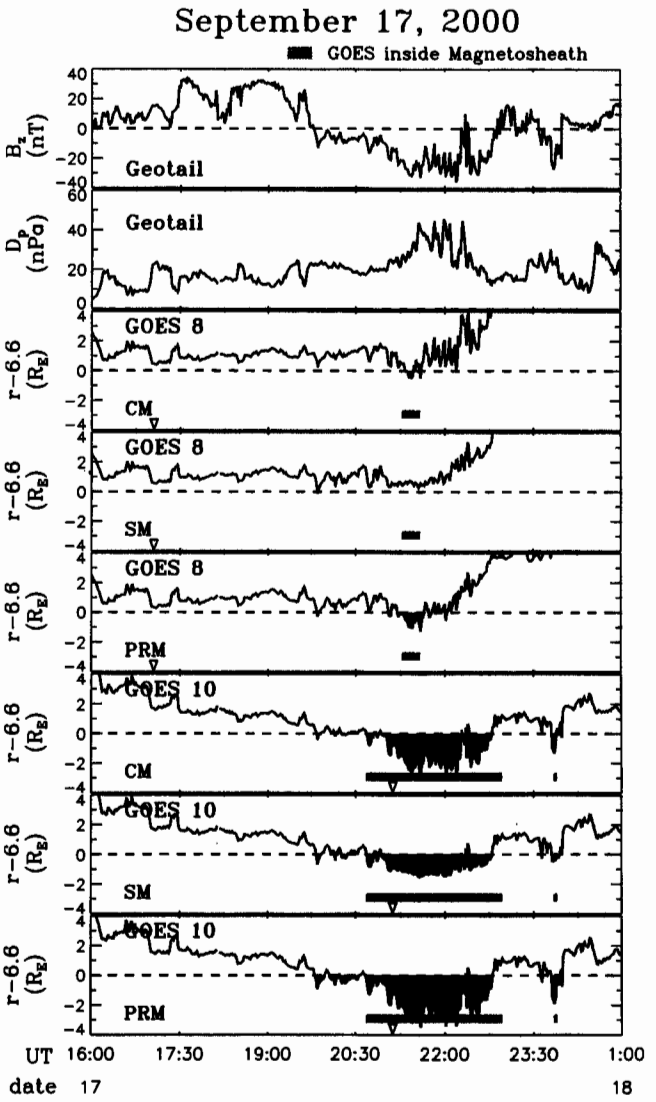

Figure 5. Comparison of predictions and observations on September 17, 2000, in the same format as Figure 3.

under the same solar wind conditions. Besides, the periods of successful forecasting for observed sheath encounters are similar for all three models. Thus it is expected that the PRM may have the largest FAT. The HTs for the three models may not be very different one another. This is consistent with the implication in Figure 1d.

[25] The forecasting results of sheath encounters at geosynchronous orbit during 1986–1992 are shown in Tables 3a and 4a. Four quantities of the three models are shown respectively in units of minutes in Tables 3a and 3b. The PRM has the largest HT and FAT as a result of more earthward magnetopause locations predicted by this model, while the CM has the smallest FAT. Tables 4a and 4b summarizes the prediction capability of these three models. The definitions of PoP, PoD, and FAR are described in section 4 and calculated from those values in Tables 3a and 3b. It shows that the PoP of the CM (79%) is the highest and that the PoD of the PRM is the highest (97%). The FARs of the CM, SM, and PRM are 69, 78, and 85%, respectively.

5.2. During 1999–2000

[26] Figures 4 and 5 illustrate the observations and predictions of April 6 and September 17, 2000, respectively, which have the

same format as Figure 3. For the April 6 event the upstream values of B_z and D_p measured by Wind, which is close to the Sun-Earth line, are used. Since the location of Wind ($X_{GSM} \sim 33\ R_E$, $Y_{GSM} \sim -233\ R_E$) is far from the Sun-Earth line on September 17, we use the data of Geotail ($X_{GSM} \sim 30\ R_E$, $Y_{GSM} \sim -2.5\ R_E$) as the upstream solar wind parameters. From Figures 4 and 5 the PRM predicts the most periods of magnetopause inside 6.6 R_E. The associated B_z and D_p values when GOES spacecraft are in the magnetosheath during 1999–2000 are plotted as pluses in Figure 6, in which the contours of $r_0 = 6.6\ R_E$ of the three models are also plotted for comparison. Those plus signs are distributed over large ranges of B_z and D_p. Tables 3b and 4b show the forecasting results of sheath encounters made by geosynchronous satellites during these two years. The PRM has the highest PoD (94%) and FAR (40%), while the CM has the highest PoP (80%) and the lowest FAR (25%). This means that most of the duration of GOES spacecraft in the magnetosheath can be predicted by the PRM, but for the warning of sheath encounters the PRM has the least reliability while the CM has the highest. However, considering the PoP, for forecasting GOES spacecraft whether in the magnetosheath or not, the CM has the best prediction.

[27] The tendency of the model's forecasting capability is similar among these three models for both periods of 1986–1992 and 1999–2000. However, the FARs of the earlier period are substantially larger than those of the later one, which is due to the larger ratio of FAT to HT during 1986–1992 than that during 1999–2000. This may be just by chance. No explicit reason can be given.

6. Discussion

[28] The radial distance r is used to check whether the magnetopause moves inside geosynchronous orbit or not, which is different from the previous [*Shue et al.*, 2000] study using r_0 instead. It is possible that the nose region of the magnetopause is within 6.6 R_E but the GOES spacecraft still stay in the magnetosphere. For example, during 1600-1800 UT on April 25, 1989, *Shue et al.* [2000] predict the GOES spacecraft should be inside the magnetosheath (see Figure 8 of *Shue et al.* [2000]), while we predict GOES 6 should be in the magnetosphere, which agrees with observations.

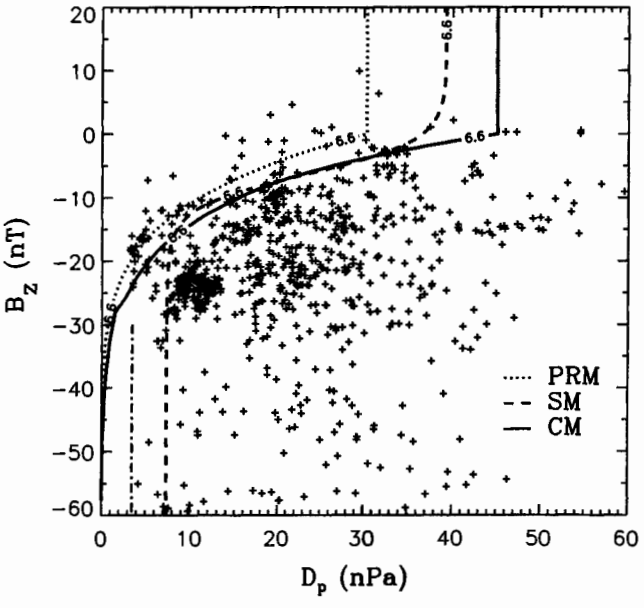

Figure 6. The IMF B_z and dynamic pressure D_p corresponding to the intervals in 1999–2000 during which GOES resided in the magnetosheath, shown with pluses. Also shown are the contours of $r_0 = 6.6\ R_E$ for the PRM, SM, and CM.

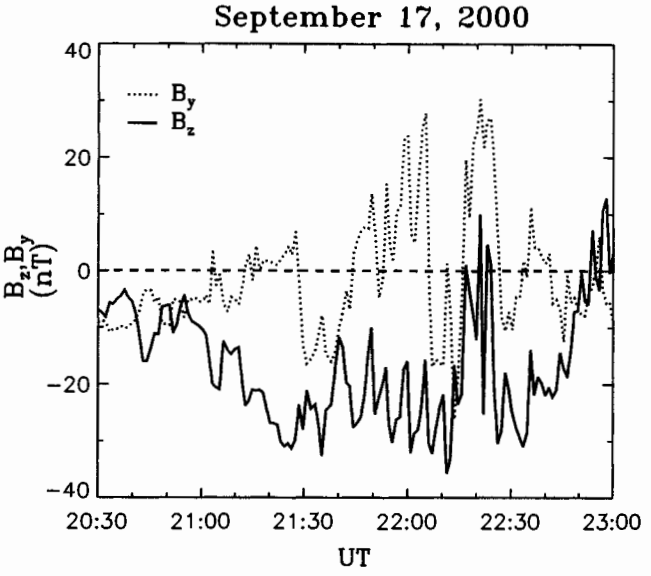

Figure 7. The IMF B_y (dotted curve) and B_z (solid curve) measured by Geotail during 2030–2300 UT on September 17, 2000.

[29] In this study the PoD and PoP never approach 100% for the SM, PRM, and CM, which is different from the results of *Shue et al.* [2000]. In their study the PoD is almost 100% for the SM and PRM; namely, nearly all geosynchronous crossings are detected by these two models. This high PoD is due to *Shue et al.*'s [2000] defined 20-min or 60-min intervals to separate two crossings. If two crossings are separated by less than 20 (or 60) min, *Shue et al.* [2000] regard them as one crossing event. When a large separating interval is used, many crossings will be included; thus the probability of detecting the crossings increases, which results in a high PoD. On the other hand, the very low values of PFP (probability of false prediction) of *Shue et al.* [2000], which means both the PRM and SM can predict crossings and noncrossings successfully, are due to the inclusion of intervals with normal solar wind conditions in their forecasting. Consequently, it is difficult to differentiate the superiority of the models during extreme conditions.

[30] In general, the periods of southward H_p observed by GOES spacecraft are taken to indicate that GOES is in the magnetosheath, but only those crossings with corresponding southward IMF B_z can be found by using magnetic field alone for identification. However, two points in Figure 1d and several points in Figure 6 are found with northward B_z, which are obtained by comparing the variations of H_p and IMF B_z. For example, southward B_z lasts a long period before 2217 UT and after 2224 UT on September 17, 2000, as shown in Figure 5, and the GOES 10 is always outside the magnetosphere. However, during 2217-2224 UT the B_z changes its direction quickly while the GOES 10 is still in the magnetosheath. This implies that the direction of IMF B_z is reversed in the magnetosheath just outside the magnetopause, especially when the B_y magnitude is much larger than the B_z magnitude. Figure 7 shows the IMF B_y and B_z measured by Geotail during 2030-2300 UT on this day. The magnitude of B_z is larger than that of B_y in most of the interval except during 2217-2224 UT when a reversed B_z is observed. Therefore we suggest that the pluses with positive B_z in Figures 1d and 6 are probably due to the magnetic field reorientation when draped over the magnetopause.

[31] For the PRM and CM a small D_p can push the magnetopause inside 6.6 R_E as long as the value of southward B_z is large enough. The r_0 predicted by SM cannot be less than 6.6 R_E when $B_z < -15$ nT unless a larger dynamic pressure exerts on the

magnetopause (i.e., $D_p > 7.5$ nPa). The distribution of pluses in the ranges $B_z < -10$ nT and $D_p < 10$ nPa shown in Figure 6 supports this tendency that the influence of southward B_z on r_0 may approach a critical value when the magnetopause is near the geosynchronous orbit. Moreover, the threshold of the southward B_z may be a function of D_p.

7. Conclusions

[32] The main conclusions are summarized as follows.

1. A database, the largest one to date, of magnetosheath encounters by geosynchronous satellites during 1986–1992 and 1999–2000 and upstream observations by Wind, IMP 8, or Geotail in the solar wind is compiled for estimating the forecasting capability of PRM, SM, and CM.

2. Higher PoP and PoD with lower FAR imply a better forecasting model. The tendency of forecasting capability of PRM, SM, and CM is similar for the periods of 1986–1992 and 1999–2000. The highest PoP of CM means this model can predict well whether the GOES is inside or outside the magnetosheath when the magnetopause's location is near 6.6 R_E. The lowest FAR of CM implies that the other two models are an overprediction for magnetosheath encounters. On the other hand, the PRM has a higher PoD, owing to its more earthward locations of magnetopause under the same solar wind conditions, while the PRM has the highest FAR.

3. From the distribution of pluses in the ranges $B_z < -10$ nT and $D_p < 10$ nPa shown in Figure 6, we propose that the subsolar magnetopause cannot be closer to the Earth when the southward IMF B_z exceeds a critical value unless a higher D_p exerts on the magnetopause. The threshold of B_z may depend on the value of D_p.

4. From the pluses with positive B_z in Figures 1d and 6, we suspect (and confirmed for one case in Figure 7) that the IMF $|B_y|$ was much larger than IMF B_z (>0). That is, the IMF was mostly horizontal, and thus the sheath field draped over the magnetopause could have a negative B_z.

[33] **Acknowledgments.** The authors thank NASA/NSSDC for providing data from the IMP 8 and Wind, and NOAA/NGDC for providing data from GOES satellites. We thank H. Sauer for providing us with some geosynchronous magnetopause crossings of GOES spacecraft. The authors also thank S. Kokubun and T. Mukai for providing the Geotail magnetic data through DARTS at the Institute of Space and Astronautical Science (ISAS) in Japan. The work was supported at UML under grant NSF-ATM-0077655. This work was supported by the National Science Council of R.O.C. under grant NSC 89-2111-M-008-019 to the National Central University and at UCLA under a grant from the National Science Foundation, AT 98-03431. Y.-H. Yang would like to thank A. V. Dmitriev for useful suggestions.

[34] Janet G. Luhmann thanks the referees for their assistance in evaluating this paper.

References

Aubry, M. B., C. T. Russell, and M. G. Kivelson, Inward motion of the magnetopause before a substorm, *J. Geophys. Res.*, *75*, 7018, 1970.

Chao, J. K., D. J. Wu, C.-H. Lin, Y. H. Yang, X. Y. Wang, M. Kessel, S. H. Chen, and R. P. Lepping, Models for the size and shape of the Earth's magnetopause and bow shock, paper presented at 2000 COSPAR Colloquium on Space Weather Study: Using Multi-Point Techniques, Comm. on Space Res., Wanli, Taipei, 2001.

Chapman, S., and V. C. A. Ferraro, A new theory of magnetic storm, I, The initial phase, *J. Geophys. Res.*, *36*, 77, 1931.

Cummings, W. D., and P. J. Coleman, Jr., Magnetic fields in the magnetopause and vicinity at synchronous altitude, *J. Geophys. Res.*, *73*, 5699, 1968.

Doswell III, C. A., R. Davies-Jones, and D. L. Keller, On summary measures of skill in rear event forecasting based on contingency tables, *Weather Forecast*, *5*, 576, 1990.

Fairfield, D. H., Average and unusual locations of the Earth's magnetopause and bow shock, *J. Geophys. Res.*, *76*, 6700, 1971.

Formisano, V., V. Domingo, and K.-P. Wenzel, The three-dimensional shape of the magnetopause, *Planet. Space Sci.*, *27*, 1137, 1979.

Holzer, R. E., and J. A. Slavin, Magnetic flux transfer associated with expansions and contractions of the dayside magnetosphere, *J. Geophys. Res.*, *83*, 3831, 1978.

Kawano, H., S. M. Petrinec, C. T. Russell, and T. Higuchi, Magnetopause shape determinations from measured position and estimated flaring angle, *J. Geophys. Res.*, *104*, 247, 1999.

Kuznetsov, S. N., and A. V. Suvorova, An empirical model of the magnetopause for broad ranges of solar wind pressure and B_z IMF, in *Polar Cap Boundary Phenomena*, edited by J. Moen et al., p. 51, Kluwer Acad., Norwell, Mass., 1998a.

Kuznetsov, S. N., and A. V. Suvorova, Solar wind magnetic field and plasma during magnetopause crossings at geosynchronous orbit, *Adv. Space Res.*, *22*(1), 63, 1998b.

McComas, D. J., S. J. Bame, B. L. Barraclough, J. R. Donart, R. C. Elphic, J. T. Gosling, M. B. Moldwin, K. R. Moore, and M. F. Thomsen, Magnetospheric plasma analyzer (MPA): Initial three-spacecraft observations from geosynchronous orbit, *J. Geophys. Res.*, *98*, 13,453, 1993.

McComas, D. J., R. C. Elphic, M. B. Moldwin, and M. F. Thomsen, Plasma observations of magnetopause crossings at geosynchronous orbit, *J. Geophys. Res.*, *99*, 21,249, 1994.

Opp, A. G., Penetration of the magnetopause beyond 6.6 R_E during the magnetic storm of January 13–14, 1967: Introduction, *J. Geophys. Res.*, *73*, 5697, 1968.

Petrinec, S. M., and C. T. Russell, An empirical model of the size and shape of the near-Earth magnetotail, *Geophys. Res. Lett.*, *20*, 2695, 1993.

Petrinec, S. M., and C. T. Russell, Near-Earth magnetotail shape and size as determined from the magnetopause flaring angle, *J. Geophys. Res.*, *101*, 137, 1996.

Petrinec, S. M., P. Song, and C. T. Russell, Solar cycle variations in the size and shape of the magnetopause, *J. Geophys. Res.*, *96*, 7893, 1991.

Roelof, E. C., and D. G. Sibeck, Magnetopause shape as a bivariate function of interplanetary magnetic field B_z and solar wind dynamic pressure, *J. Geophys. Res.*, *98*, 21,421, 1993.

Rufenach, C. L., R. F. Martin, Jr., and H. H. Sauer, A study of geosynchronous magnetopause crossings, *J. Geophys. Res.*, *94*, 15,125, 1989.

Russell, C. T., On the occurrence of magnetopause crossings at 6.6 R_E, *Geophys. Res. Lett.*, *3*, 593, 1976.

Schaefer, J. T., The critical success index as an indicator of warning skill, *Weather Forecast*, *5*, 570, 1990.

Shue, J.-H., J. K. Chao, H. C. Fu, C. T. Russell, P. Song, K. K. Khurana, and H. J. Singer, A new functional form to study the solar wind control of the magnetopause size and shape, *J. Geophys. Res.*, *102*, 9497, 1997.

Shue, J.-H., et al., Magnetopause location under extreme solar wind conditions, *J. Geophys. Res.*, *103*, 17,691, 1998.

Shue, J.-H., P. Song, C. T. Russell, J. K. Chao, and Y.-H. Yang, Toward predicting the position of the magnetopause within geosynchronous orbit, *J. Geophys. Res.*, *105*, 2641, 2000.

Sibeck, D. G., R. E. Lopez, and E. C. Roelof, Solar wind control of the magnetopause shape, location, and motion, *J. Geophys. Res.*, *96*, 5489, 1991.

J. K. Chao, C.-H. Lin, and Y.-H. Yang, Institute of Space Science, National Central University, Chung-Li, Taiwan. (yhyang@jupiter.ss.ncu.edu.tw)

A. J. Lazarus, Center for Space Research, Massachusetts Institute of Technology, 77 Massachusetts Avenue, Cambridge, MA 02139, USA.

R. P. Lepping, Laboratory for Extraterrestrial Physics, NASA Goddard Space Flight Center, Code 696.0, Greenbelt, MD 20771, USA.

C. T. Russell, Institute of Geophysics and Planetary Physics, University of California, Los Angeles, CA 90095-1567, USA.

J.-H. Shue, Applied Physics Laboratory, Johns Hopkins University, Laurel, MD 20723-6099, USA.

P. Song, Center for Atmospheric Research, University of Massachusetts, Lowell, MA 01854, USA.

X.-Y. Wang, Center for Space Science and Applied Research, Academic Sinica, Beijing, China.